

Multifunction Myoelectric Control using Multi-Dimensional Dynamic Time Warping

Meena AbdelMaseeh, Tsu-Wei Chen, and Daniel Stashuk

Abstract—Myoelectric control can be used for a variety of applications including powered prostheses and different human computer interface systems. The aim of this study is to investigate the formulation of myoelectric control as a multi-class distance-based classification of multidimensional sequences. More specifically, we investigate (1) estimation of multi-muscle activation sequences from multi-channel electromyographic signals in an online manner, and (2) classification using a distance metric based on multi-dimensional dynamic time warping. Subject-specific results across 5 subjects executing 10 different hand movements showed an accuracy of 95% using offline extracted trajectories and an accuracy of 84% using online extracted trajectories.

I. INTRODUCTION

Advancements in instrumentation and microprocessor technologies have allowed the realization of portable systems capable of acquiring and analyzing multi-channel electromyographic signals in real-time. Such systems can be used for a wide variety of applications including the control of powered prostheses [5] and human computer interfaces [6]. The formulation of myoelectric control as the multi-class classification of multidimensional sequences allows extension to multifunction control, where the number of the functions controlled can exceed the number of channels of EMG signals acquired. Sequence classification methods can be grouped into 3 main categories [9]:

- Feature-based: A feature vector of a fixed length is extracted to represent the sequence.
- Distance-based: A metric is defined to measure the similarity between a pair of indices across a pair of sequences.
- Model-based: Sequences are classified based on how well they fit an assumed model.

This work adopts the formulation of myoelectric control as a multi-class classification problem. Specifically, a distance-based classification method is investigated. To the best of our knowledge, this category of methods has not been previously investigated for myoelectric control.

In this work, a specific multi-muscle activation sequence is presumed to be mapped to a specific control function. The multi-channel EMG activation-level signals associated with a multi-muscle-activation sequence are referred to as a trajectory and dynamic time warping (DTW) is used as a distance measure between two trajectories. DTW is used as a distance because it:

- matches sequences of different lengths and therefore there is no additional step required to convert the trajectories into another form.
- is indifferent to the speed with which a multi-muscle activation sequence is performed as well as non-linear distortions as shown in Figure 1.

A comprehensive survey of 8 common similarity measures applied to 38 different data sets from a wide variety of application domains showed supporting evidence that DTW is the best distance measure for most domains [1]. Classification based on multidimensional DTW (MD-DTW) was also shown to perform as well as or to outperform classification based on single-channel DTW [7].

In addition, the system presented here is expected to be flexible. For the signals evaluated, electrode placement did not assume careful placements such that each electrode was associated with a particular muscle(s) and the methods are designed to account for potential electrode movement. This allows the electrodes to be easily applied/reapplied for signal acquisition without the need for precise alignment with anatomical landmarks.

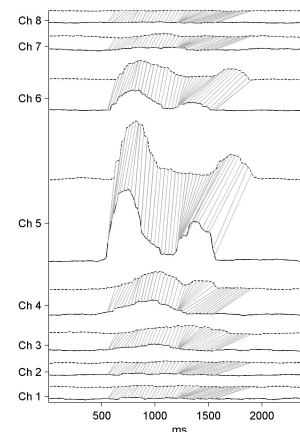


Fig. 1. Example showing how dynamic time warping accommodate to variations in the speeds of hand movement execution. Two trajectories representing the same movement as executed by the same subject are interleaved together. One trajectory is represented with dotted lines, while the other trajectory is represented with solid line. The gray lines represent every 15th alignment from one time instance of a trajectory to a time instance in the other trajectory. In particular, in channel 5, it can be observed that the dashed trajectory is corresponding to a slower movement. DTW is shown to be able to account for this by aligning many time instances from the trajectory corresponding to the slower movement to a single time instance in the other trajectory.

The authors are with the department of Systems Design Engineering, University of Waterloo, Waterloo, ON, Canada stashuk at uwaterloo.ca

II. METHODOLOGY

A. System Overview

The information flow of the proposed system is shown in Figure 2. Surface EMG signals are obtained from multiple surface channels, say q . The signals are then preprocessed to accentuate the electrophysiological contributions of interest relative to other signals and noise. The preprocessed signals are then rectified, smoothed and normalized to obtain a multi-dimensional activation-level signal $A(t) = \langle a_1(t), \dots, a_i(t), \dots, a_q(t) \rangle$. Each element in $A(t)$ is expected to be correlated to the level of contraction of a group of the muscles that are relatively close to the detection surface of the corresponding electrode.

The i^{th} channel is assumed to be active at a given sample t , if the activation-level $a_i(t)$ is significantly different from the background activity. Still, a multi-muscle activation sequence is only assumed to have occurred when a number of channels are detected to be simultaneously active for a continuous period of time.

Trajectory X is defined as the activation-level signals obtained from the q channels between the detected onset sample t_0 and the end sample t_f after being smoothed and circular shifted.

For an application with m distinct control functions, a training set $R = \{(X_1, y_1), \dots, (X_l, y_l), \dots, (X_n, y_n)\}$ is comprised of n labeled trajectories, where $y_l \in \{c_1, \dots, c_m\}$ is the label of trajectory X_l . In order to classify an unlabeled trajectory, say X_k , the distance $\Psi(X_l, X_k)$ based on MD-DTW is calculated between X_l and each of the n labeled trajectories. The label y_k is set to the label of the trajectory found to be closest to X_k .

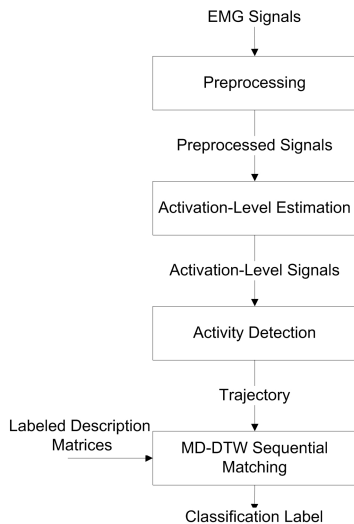


Fig. 2. Information flow of the proposed system

B. Preprocessing

A high-pass Butterworth filter with corner frequency at 20 Hz and a 12 dB/octave roll-off is utilized for preprocessing. It was shown in [4] that using a filter with this configuration

results in the best trade off between preserving EMG content and eliminating artifacts due to electrode movement. Also, high-pass filtering is expected to reduce crosstalk [8] by attenuating contributions from muscle fibers distant from the electrode.

C. Activation-Level Estimation

An activation-level signal (i.e. a signal related to the level of activation of a muscle) can be calculated using a surface detected EMG signal recorded from the active muscle using the general schema of decoding, smoothing and relinearization [2]. In this work, an activation-level signal is calculated as the root-mean-square (rms) value of the preprocessed EMG signal, which is equivalent to decoding using squaring, smoothing by averaging over a moving window of length ϵ , and relinearization by taking the square root. Activation-level signals were shown to be correlated to the level of muscle contraction [3], since they are related to how many motor units are recruited and their mean firing rates.

The characteristics of the background activity are then captured by calculating the mean $\mu_{rest} = \langle \mu_{rest}(1), \dots, \mu_{rest}(q) \rangle$ and the standard deviation $\sigma_{rest} = \langle \sigma_{rest}(1), \dots, \sigma_{rest}(q) \rangle$ of the rms signals of training examples labeled as "rest". In order to obtain an activation level-signal, the rms signal of each channel is divided by its corresponding $\mu_{rest}(i)$.

D. Activity Detection

The sample $a_i(t)$ of an activation-level signal is assumed to be "active", if $a_i(t) \geq \frac{\gamma \sigma_{rest}(i)}{\mu_{rest}(i)}$. As will be explained later, the sample activity factor γ is induced using a training set R so as to minimize confusion between examples labeled as rest and other examples.

Extraction of a trajectory (i.e., detection of its onset t_0 and end t_f) is challenging because:

- The detection of a few isolated active samples does not necessarily indicate the execution of a multi-muscle activation sequence, since this activity is more likely to be due to noise or electrode movement.
- The activation trajectory of a multi-muscle activation sequence can be multi-phasic, meaning that it may include more than one burst of activity separated by rest. Therefore, the detection of rest following an activity may not be suitable for the detection of t_f .

In this study, two techniques for detecting t_0 and t_f were investigated:

1) *Offline Trajectory Extraction*: For a given epoch of multi-channel EMG activation-level signals, t_0 is set to the first sample at which a channel or more are detected to be active, and similarly t_f is set to the last sample. This technique is not suitable for applications requiring online myoelectric control and hence its name. It also assumes that a single multi-muscle activation sequence is included in each epoch. On the other hand, the main advantage of this technique is that it has no problem extracting multi-phasic trajectories.

2) *Online Trajectory Extraction*: This technique can be used for online extraction of trajectories (i.e., myoelectric control) and is capable of detecting successive trajectories from a streaming signal. As the sample t arrives, the number of active channels $u(t)$ is estimated using a window spanning from $t - \tau$ to t . A channel is considered to be active and consequently $u(t)$ is incremented, when the ratio of active samples in the window to τ is above the threshold δ .

Four events need to occur in the following order for a trajectory to be detected:

- 1) $u(t)$ exceeds a preset minimal number of channels α .
- 2) $u(t)$ stays above α for τ_{active} samples.
- 3) $u(t)$ goes below α .
- 4) $u(t)$ stays below α for $\tau_{inactive}$ samples.

For either the online or offline trajectory extraction techniques, the sample activity factor γ is set to an integer between 1 and 30 that minimizes the confusion in a training set defined as the sum of (1) the number of times that a trajectory is detected in a training set trial labeled as rest and (2) the number of times that no trajectory is detected in a training set trial that is not labeled as rest. For each value of γ (between 1 and 30), the trajectory extraction technique is applied and the confusion is calculated. γ is set to the middle of the range over which the confusion is minimal.

Each extracted trajectory is decimated by the factor β . The decimation is preceded by low-pass filtration to diminish frequency components exceeding $\frac{F_s}{2 \times \beta}$ yielding a trajectory indexed by \bar{t} from \bar{t}_0 to \bar{t}_f .

In order to count for misalignment or movement of the electrodes, the rows of the decimated trajectories are circularly shifted by one in both directions yielding a trajectory represented using a matrix $X \in M_{q \times (\bar{t}_f - \bar{t}_0) \times 3}$. The trajectory has q rows (the number of channels), $(\bar{t}_f - \bar{t}_0)$ columns (the number of samples after decimation), and a depth of 3 (the number of circular shifts).

E. Matching Using Multidimensional Dynamic Time Warping

MD-DTW is used to align two trajectories at a given circular shift, say χ_k and χ_l , diminishing the effects of different execution speeds of the respective multi-muscle activation sequences. Let the number of decimated samples in χ_k and χ_l to be λ_k and λ_l , respectively. Also, let the alignment between two arbitrary samples from the two trajectories, say $\chi_k(:, \bar{t}_a)$ and $\chi_l(:, \bar{t}_b)$, be denoted as $w = \langle a, b \rangle$ and the distance associated with this alignment be the Euclidean distance between the two samples $d(w)$.

MD-DTW searches for a path (i.e., a sequence of alignments between pairs of samples $P = \langle w(1), \dots, w(j), \dots, w(|P|) \rangle$) that minimizes the accumulated distance defined as: $\rho(\lambda_k, \lambda_l) = \sum_{j=1}^{|P|} d(w(j))$ subject to the following conditions:

- **Boundary**: $w(1) = \langle 1, 1 \rangle$ and $w(|P|) = \langle \lambda_k, \lambda_l \rangle$.
- **Monotonicity**: If $w(j) = \langle a, b \rangle$ and $w(j+1) = \langle c, d \rangle$, then $c \geq a$ and $d \geq b \forall j$.
- **Step size**: If $w(j) = \langle a, b \rangle$ and $w(j+1) = \langle c, d \rangle$, then $c - a \leq 1$ and $d - b \leq 1 \forall j$.

The search for the path P can be obtained using dynamic programming. Let $P(a, b)$ be the optimal path from $\langle 1, 1 \rangle$ to $\langle a, b \rangle$ that minimizes the accumulated distance $\rho(a, b)$ obtained using the following recursive formula:

$$\rho(a, b) = d(a, b) + \min(\rho(a-1, b-1), \rho(a, b-1), \rho(a-1, b)) \quad (1)$$

Deletion of a point in χ_k with respect to χ_l occurs when $\min(\rho(a-1, b-1), \rho(a, b-1), \rho(a-1, b)) = \rho(a-1, b)$. Insertion of a point in χ_k with respect to χ_l occurs when $\min(\rho(a-1, b-1), \rho(a, b-1), \rho(a-1, b)) = \rho(a, b-1)$. In order to discourage large time differences in the alignments, insertions and deletions are weighted differently in Equation 2:

$$\rho_\zeta(a, b) = d(a, b) + \min(\rho_\zeta(a-1, b-1), \zeta \rho_\zeta(a, b-1), \zeta \rho_\zeta(a-1, b)) \quad (2)$$

where $\zeta > 1, \zeta \in \mathbb{R}$.

In this work, the distance between χ_k and χ_l was defined as $\psi(\chi_k, \chi_l) = \frac{\rho_\zeta(\lambda_k, \lambda_l)}{|P|}$. The normalization is necessary to account for the fact that matching different trajectories is expected to result in paths having different lengths.

The MD-DTW accumulated distance between two trajectories is obtained as $\psi(X_k, X_l) = \min_{s=-1,0,1}(\psi(X_k(:, :, s), X_l(:, :, 0)))$, i.e., the minimum distance obtained from matching the depth of trajectory $X_l(:, :, 0)$, representing no circular shift, to each of the depths of $X_k(:, :, s)$ representing no shift and shifts of ± 1 . The distances between an unlabeled trajectory and all labeled trajectories belonging to R are calculated sequentially. The label of the unlabeled trajectory is then assigned to the label of the closest labelled trajectory.

III. EMPIRICAL EVALUATION

An armband including 8 equally spaced surface electrodes was placed around the right forearm. Five subjects participated in this experiment. At the beginning of each trial, the subject had his hand at rest. An instruction to perform a specific hand movement was then displayed on a screen placed in front of the subject followed by an instruction to return to rest again. The 9 tested hand movements were finger tap, right, left, swipe up, swipe down, swipe right, swipe left, gun, and fist. The subject was required to perform 10 trials for each hand movement. In another 10 trials, the subject was required to keep his hand at rest. The signals were sampled at 300 HZ.

The trials collected from each subject were dealt with as a separate dataset. This means that for cross validation testing, the trials used for testing were collected from one subject and matched to trials collected from the same subject. 10 fold stratified cross validation was used, i.e., 10% of the trials used for testing in each fold were chosen to belong to different hand movements. For online trajectory extraction, the trials used for testing were randomly concatenated to simulate a random sequence of hand movements. μ_{rest} , σ_{rest} , and γ were re-estimated in each fold for either online

or offline trajectory extraction. Classification accuracies obtained using offline trajectory extraction and online trajectory extraction are given in Table I.

TABLE I

ACCURACY OF HAND MOVEMENT RECOGNITION FOR DIFFERENT SUBJECTS BASED ON OFFLINE AND ONLINE TRAJECTORY EXTRACTION.

Trajectory Extraction	Average Over Trials					Average Over Subjects (%)
	S1 (%)	S2 (%)	S3 (%)	S4 (%)	S5 (%)	
Offline	88	97	96	97	99	95
Online	67	92	73	98	90	84

IV. DISCUSSION

The results presented in Tables I show the ability of the MD-DTW accumulated distance ψ to discriminate between the trajectories of different hand movements performed by the same subject. This performance can be attributed to the following reasons:

- 1) Activation-level signals disregard non-discriminative aspects of EMG signals, such as the morphology of constituent motor unit potentials. This results in smoother and more discriminative trajectories.
- 2) MD-DTW is capable of accurately aligning trajectories of the same hand movement executed at different speeds.
- 3) MD-DTW is tolerant to temporally limited local variations in the trajectories, because the sequence of alignments is selected to optimize the accumulated distance over the complete lengths of the 2 matched trajectories for all channels.
- 4) MD-DTW is capable of diminishing the effects of irrelevant and/or mistakenly detected activities.

The discriminability provided by the proposed distance metric was investigated using trajectories extracted based on both online and offline extraction techniques. The trajectories extracted offline are expected to be more complete, since offline extraction has no problem with trials that have more than one phase. This can explain the 11% improvement on average compared to online extracted performance. There are three likely reasons that can explain this decrease in accuracy using online trajectory extraction:

- 1) failure of the online trajectory extraction technique to link the phases in a given trial
- 2) inaccuracy of the detected onset and the end positions
- 3) propagation of error, i.e., an error in trajectory extraction and/or matching to the correct hand movement results in an error in matching the following concatenated trial

The degree of variability across subjects is also clear in Table I. Specifically, the first subject clearly produced the least consistent activation trajectories. This can be explained to some extent by the observation that online trajectory extraction detected a single trajectory in only 76% of the subject's trials

The online extraction technique was tested by creating simulated signals formed by concatenating randomly selected trials. This might not represent the situation in which a subject does not rest after the execution of each hand movement. However, the use of the simulated signal allows indirect investigation of (1) the possibility of detecting more than one hand movement from a given signal, and (2) the likelihood of detecting more than one phase in one trial.

There is no confusion between rest and non-rest trials for either online or offline extraction techniques. This suggests that the activation-level signal is correlated to the level of muscle contraction as assumed. It also suggests that the use of a wrapper search to set the standard deviation δ factor is effective.

V. CONCLUSION

This work demonstrates the potential utility of using distance-based classification methods with multidimensional sequences in the context of myoelectric control. Accumulated distance based on MD-DTW alignments was shown to be a particularly discriminative measure across trajectories corresponding to different hand movements. An accuracy of 95% was achieved based on trajectories obtained using the offline extraction technique. In order to step towards the realization of online myoelectric control, we proposed an online trajectory extraction technique. However, an 11% decrease in accuracy was observed compared to the use of offline trajectory extraction, which indicates the need for improving the existing method for online trajectory extraction.

REFERENCES

- [1] Hui Ding, Goce Trajcevski, Peter Scheuermann, Xiaoyue Wang, and Eamonn Keogh. Querying and mining of time series data: experimental comparison of representations and distance measures. *Proceedings of the VLDB Endowment*, 1(2):1542–1552, 2008.
- [2] Dario Farina, Roberto Merletti, and Roger M. Enoka. The extraction of neural strategies from the surface emg. *Journal of Applied Physiology*, 96(4):1486–1495, 2004.
- [3] Verne T. Inman, H. J. Ralston, J. B. De C. M. Saunders, M. B. Bertram Feinstein, and Elwood W. Wright Jr. Relation of human electromyogram to muscular tension. *Electroencephalography and Clinical Neurophysiology*, 4(2):187 – 194, 1952.
- [4] Carlo J. De Luca, L. Donald Gilmore, Mikhail Kuznetsov, and Serge H. Roy. Filtering the surface emg signal: Movement artifact and baseline noise contamination. *Journal of Biomechanics*, 43(8):1573 – 1579, 2010.
- [5] P. Parker, K. Englehart, and B. Hudgins. Myoelectric signal processing for control of powered limb prostheses. *Journal of Electromyography and Kinesiology*, 16(6):541 – 548, 2006.
- [6] T. Scott Saponas, Desney S. Tan, Dan Morris, Jim Turner, and James A. Landay. Making muscle-computer interfaces more practical. In *Proceedings of the SIGCHI Conference on Human Factors in Computing Systems*, CHI '10, pages 851–854, New York, NY, USA, 2010. ACM.
- [7] GA Ten Holt, MJT Reinders, and EA Hendriks. Multi-dimensional dynamic time warping for gesture recognition. In *Thirteenth annual conference of the Advanced School for Computing and Imaging*, volume 300, 2007.
- [8] D. A. Winter, A. J. Fuglevand, and S. E. Archer. Crosstalk in surface electromyography: Theoretical and practical estimates. *Journal of Electromyography and Kinesiology*, 4(1):15 – 26, 1994.
- [9] Zhengzheng Xing, Jian Pei, and Eamonn Keogh. A brief survey on sequence classification. *SIGKDD Explor. Newsl.*, 12(1):40–48, November 2010.